Research Article Vol. 28, No. 12 / 8 June 2020 / Optics Express 17532

Optics EXPRESS

Room temperature quantum cascade lasers with 22% wall plug efficiency in continuous-wave operation

F. WANG, S. SLIVKEN, D. H. WU, AND M. RAZEGHI*

Center for Quantum Devices, Department of Electrical and Computer Engineering, Northwestern University, Evanston, IL 60208, USA

*razeghi@northwestern.edu

Abstract: We report the demonstration of quantum cascade lasers (QCLs) with improved efficiency emitting at a wavelength of 4.9 µm in pulsed and continuous-wave (CW) operation. Based on an established design and guided by simulation, the number of QCL-emitting stages is increased in order to realize a 29.3% wall plug efficiency (WPE) in pulsed operation at room temperature. With proper fabrication and packaging, a 5-mm-long, 8-µm-wide QCL with a buried ridge waveguide is capable of 22% CW WPE and 5.6 W CW output power at room temperature. This corresponds to an extremely high optical density at the output facet of ~35 MW/cm^2, without any damage.

1. Introduction

The quantum cascade laser (QCL) is a semiconductor device based on intersubband transitions [1]. After more than twenty-five years of development, it has become the most important coherent source of light in mid-infrared and terahertz (THz) ranges [2–8]. The wall-plug efficiency (WPE) of a QCL represents the energy conversion efficiency from electrical power input to optical power output. Optimizing the WPE can not only efficiently take advantage of electrical energy, but also can minimize the waste heat produced within a laser, which can significantly improve the reliability of lasers, especially for QCLs under continuous-wave (CW) operation. Unlike traditional semiconductor lasers whose WPE is capable of exceeding ~70% at room temperature [9], it has proven to be challenging to improve the WPE of a QCL since a minimum voltage (typically above 10 V) is required to align the cascade structures before any gain behavior. Besides, lower quantum efficiency and stronger carrier thermalization during electron transport in minibands also prevent the increase of QCL WPE. In 2011, a high performance QCL with ~21% WPE in CW operation and ~27% WPE in pulsed operation was demonstrated at room temperature by Bai *et al.* [10]. This laser, based on the shallow-well design [11], consists of 40 QCL-stages and is featured by a high characteristic temperature $T_0 \approx 240$ K. Since then, no improvement of the CW WPE of QCLs has been reported. Although a newly designed QCL with ~28% pulsed WPE was demonstrated a few years ago, its CW performance is far below 21% due to a significantly lower characteristic temperature of $T_0 \approx 140$ K [12].

In fact, without modifying the band structure of a QCL, its pulsed WPE can be also improved by increasing the thickness of the laser core (proportional to the number of QCL stages, N_s) as it can raise the waveguide optical confinement factor (Γ), reduce the waveguide loss (α_w), and lower the threshold current density (J_{th}). Lower waveguide loss permits increasing the WPE ($\eta_{\rm wpe}$) by lifting the optical efficiency ($\eta_{\rm o}$) since $\eta_{\rm wpe} = \eta_{\rm o} \cdot \eta_{\rm i} \cdot \eta_{\rm v} \cdot \eta_{\rm e}$ and $\eta_{\rm o} = \alpha_{\rm m}/(\alpha_{\rm m}+\alpha_{\rm w})$, where $\eta_{\rm i}$, $\eta_{\rm v}$, $\eta_{\rm e}$, $\alpha_{\rm m}$ is the internal quantum efficiency, voltage efficiency, electrical efficiency and mirror loss, respectively [2]. A higher confinement factor enables WPE improvement by decreasing the threshold current density, because less gain (g) is required to for lasing ($g = (\alpha_{\rm m}+\alpha_{\rm w})/\Gamma$). However, increasing N_s will also increase the temperature of the laser core in CW operation,

#394916 https://doi.org/10.1364/OE.394916
Journal © 2020 Received 10 Apr 2020; revised 11 May 2020; accepted 12 May 2020; published 27 May 2020

Optics EXPRESS

which will strongly degrade the performance. Thus, in order to achieve higher CW WPE, a compromise between the thickness increase and thermal accumulation is required.

In this paper, we firstly study the feasibility of increasing the CW WPE of mid-infrared QCLs using optical and thermal simulations. Then, we take the design with the current state-of-the-art performance as a Ref. [10]. By increasing the QCL-stages from 40 to 45 and improving the quality of processing, we demonstrate a QCL, emitting at ~4.9 µm, which demonstrates the highest room temperature, pulsed WPE to date (29.3%). This design is also shown to be capable of delivering 5.6 W optical power in CW operation from a single facet with an unprecedented WPE of 22%. An extremely high optical power density of ~35 MW/cm^2 has been achieved at room temperature without damaging the outcoupling facet. This result achieves an important milestone in CW QCL efficiency and output power and demonstrates the reproducibility of material growth and device fabrication quality.

2. Optical simulation

Firstly, we numerically studied the influence of N_s on α_w and Γ. The buried ridge waveguide QCL with a ridge with of 8 µm is modeled as Fig. 1(a). From bottom to top, it is the substrate (InP), buffer layer (n- InP), laser core (GaInAs/AlInAs), cladding layer (n- InP), cap layer (n+ InP), isolation layer (SiO_2) and top contact (Au), respectively. Their thickness from buffer to top contact are set to be 1 µm, 0.44*N_s µm, 3 µm, 1 µm, 0.5 µm and 3 µm, respectively, and the window opening is chosen to be 2 µm. On either side of the laser core is a semi-insulating InP layer, which is regrown during the laser fabrication. Although there is a bottom contact layer (Ge/Au, Ni, Au) in a real QCL device below the substrate, its effect on the optical mode is negligible since the thickness of InP-based substrate is more than 100 µm. So, the bottom contact is not taken into account in the optical modelling.

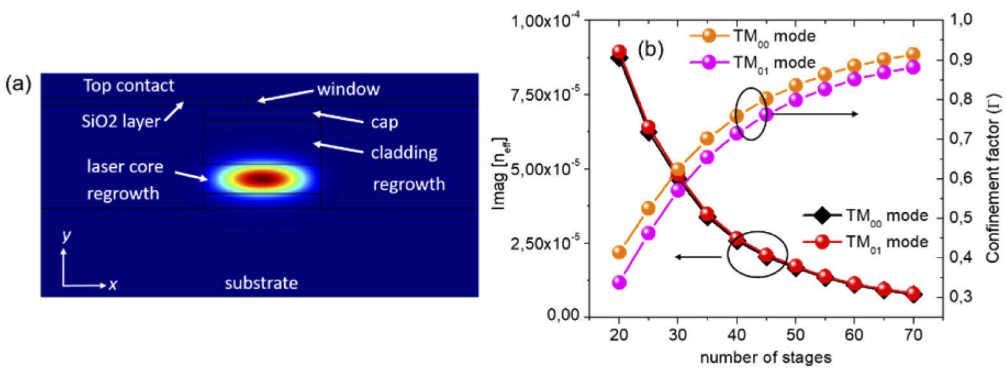

Fig. 1. (a) The optical modal simulation of a buried ridge QCL. (b) The imaginary part of the effective refractive index (proportional to waveguide loss) and the confinement factor of the buried QCL as a function of the numbers of QCL stages.

Based on the model, we calculated α_w and Γ for the fundamental mode (TM_{00}) and high order transverse mode (TM_{01}) of the buried ridge QCL as a function of N_s from 20 to 70. As shown in Fig. 1(b), between $N_s = 20$–45, the waveguide loss and confinement factor change rapidly with the increase of QCL stages, while between $N_s = 45$–70, both curves start to converge towards a constant. If N_s is increased from 40 to 45, the waveguide loss will decrease by more than 27% for both TM_{00} and TM_{01} modes. For a 5-mm-long mid-infrared QCL, the mirror loss is $\alpha_m = ln(1/R_1 \cdot R_2)/2L \approx 2.6$ cm^{-1}. Taking the estimated $\alpha_w \approx 0.5$ cm^{-1} from Ref. [10], the stage change will lead to an improvement of optical efficiency from ~84% to ~88%.

Optics EXPRESS

For a QCL, the threshold current density J_{th} can be expressed as Eq. (1) [13]:

$$J_{th} = J_{tr} + \frac{\alpha_m + \alpha_w}{g_d \Gamma} \tag{1}$$

where J_{tr} is the transparency current density and g_d is the material differential gain. Both are assumed to be constant with respect to N_s. From cavity-length dependent testing of the laser from Ref. [10], J_{tr} and $g_d\Gamma$ are estimated to be 0.72 kA/cm^2 and 4.7 cm/kA, respectively. As shown in Fig. 1(b), when increasing N_s from 40 to 45, the confinement factor is increased from ~0.75 to ~0.80 for the TM_{00} mode and increased from ~0.71 to ~0.76 for the TM_{01} mode. This results in a decrease of threshold current density by 4.9%.

A simplified expression for the WPE can be written as:

$$\eta_{wpe} = \eta_s \frac{(J - J_{th})}{J \cdot V} = \frac{\hbar\omega N_s}{qV} \eta_i \eta_o \frac{(J - J_{th})}{J} \tag{2}$$

where η_s is the slope efficiency, J is the operating current density, V is the applied voltage, and $\hbar\omega$ is the photon energy. It is assumed that V roughly scales proportionally to N_s, which simplifies analysis. From Ref. [10], the maximum WPE occurred for J = 4.25 kA/cm^2. Based on estimates for the η_o and J_{th} given above, increasing N_s from 40 to 45 should increase the WPE to ~28.9%.

3. Thermal simulation

Although the WPE increases with N_s owing to the improvement of waveguide loss and confinement factor, the temperature of the laser core for the same input power density also increases rapidly. This heating is significant for CW operation lasers and will drag back the WPE due to enhanced non-radiative relaxation and reduced transport efficiency [14]. As such, the thickness increase of the laser core cannot guarantee the increase of CW WPE and the thermal issues have to be taken into account.

The buried ridge epi-down bonded mid-infrared QCL under CW operation is modelled as Fig. 2(a). Similar to the optical modeling, from bottom to top in order, it is InP substrate, highly doped buffer layer, InGaAs/AlInAs laser core, InP cladding and cap layer, SiO_2 isolation layer, top contact (gold). In addition, an indium layer and a diamond heat spreader are added on the top contact for efficient heat removal under CW operation. As a boundary condition, the temperature of the top surface of the diamond heat spreader is set to be kept as constant (300 K). Heat transfer in QCL is described using Eq. (3) [15]:

$$\nabla \cdot [k(x, y, T)\nabla T(x, y, t)] + S(x, y, t) = 0 \tag{3}$$

where $T(x,y)$ is the temperature distribution, k is the thermal conductivity of materials under consideration, and S is the power density of heat source. In this model, the laser core is supposed to be the only heat source. As shown in Fig. 2(b), the maximum (T_{max}) and average ($T_{average}$) temperature of laser core under CW operation are simulated as a function of N_s for a constant power density ($S = 2.3 \times 10^{14}$ W/m^3). Above 30 stages, the increase is approximately linear. From 40 to 45, T_{max} is increased by 20 °C from 394 K to 414 K and T_{ave} is increased by 10°C from 355 K to 365 K.

The temperature dependence of WPE can be obtained from Eq. (2) by substituting $J_{th} = J_0 \cdot exp(T/T_0)$ and $\eta_s = \eta_{s0} \cdot exp(-T/T_1)$, where T is the average core temperature, $T_0 \approx 220$ - 250 K is the characteristic temperature for threshold, J_0 is the extrapolated J_{th} at 0 K, $T_1 \approx 400$ - 500 K is the characteristic temperature for slope efficiency, and η_{s0} is the extrapolated η_s at 0 K. Based on the thermal simulation values for the 40 stage core and the pulsed WPE (27%) from Ref. [10], the CW WPE is estimated to drop to ~21%, which matches very well to the CW testing results in the same reference. As N_s increases to 45, J_{th} increases by another 4.2% and η_s drops by 2.3%, which from Eq. (2) leads to a CW WPE estimate of 21.7% for the same waveguide geometry and power density.

Optics EXPRESS

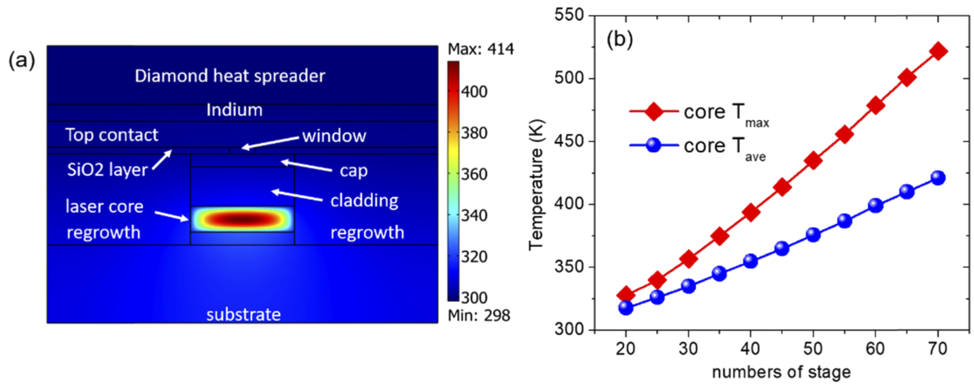

Fig. 2. (a) The model and temperature distribution of a buried ridge QCL epi-down bonded on a diamond heat spreader for CW operation. (b) The maximum (T_{max}) and average ($T_{average}$) core temperature of the buried ridge QCL under CW operation as a function of QCL stages.

4. Experiments

Based on the shallow-well design in Refs. [10,11], the new QCL wafer was grown in a gas-source molecular beam epitaxy (GSMBE) reactor on n-InP substrate. As shown in Fig. 3(a), it consists of 45 QCL stages and ends with a 3-µm low doped (2×10^{16} - 2×10^{17} cm^{-3}) InP cladding layer and a 1-µm highly doped (1×10^{19} cm^{-3}) InP cap layer. The laser core doping concentration is nominally the same as the laser from Ref. [10]. A dark field optical microscope image of the wafer surface is shown in the lower part of Fig. 3(a) which indicates the wafer has a defect density below 1.1×10^5 cm^{-2}. Figure 3(b) shows the photoluminescence of the new and reference wafers at room temperature. The peak of the spectrum is centered at $\lambda = 1434$ nm with a full width at half max (FWHM) of ~34 meV. Compared with the wafer in Ref. [10], they are almost

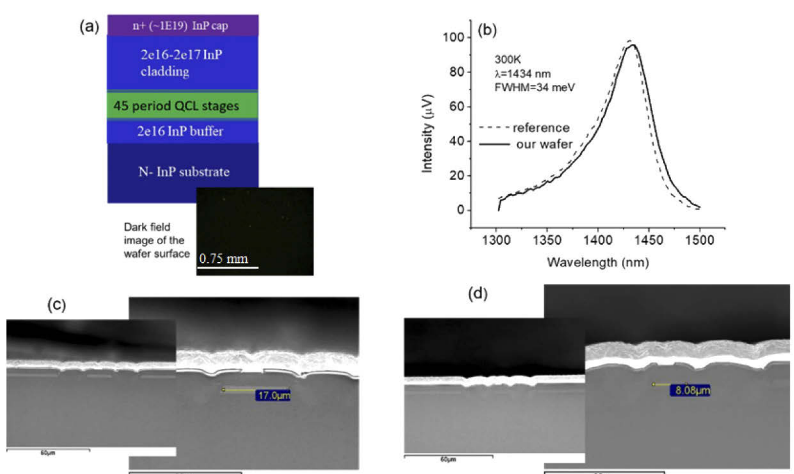

Fig. 3. (a) The QCL wafer grown structure (upper) and the dark field of the wafer surface after growth (lower). (b) The photoluminescence of the wafer and comparison with the reference wafer. (c) The SEM images of the cross section of buried ridge QCL device with a wide ridge width for pulsed operation. (d) The SEM images of the cross section of buried ridge QCL device with a narrow ridge width for CW operation.

Optics EXPRESS

overlapped, which shows that material composition, thickness, and quality for the two wafers are comparable and highlights the reproducibility of the active material growth.

We firstly processed this wafer as a buried ridge waveguide with a wide ridge width of ~17 µm as shown in Fig. 3(c). This wide ridge width gives better uniformity across the processed wafer and allows for an accurate estimation on the important parameters of the material and device such as J_{tr}, $g_d\Gamma$, α_w, and η_i. To improve the reliability of QCLs, an improved device geometry was developed, based on the flattest possible regrowth surface as shown in Figs. 3(c) and (d). This improved device fabrication process provides the most consistent performance and facilitates void-free epi-layer-down bonding for CW operation.

Figure 4(a) shows the power-current-voltage (LIV) characteristics and extracted WPE of a 5 mm, uncoated laser. The measurement was conducted in pulsed mode with a pulse width of 500 ns and a duty cycle of 2% on a stage held at 293 K. The threshold current density is 1.22 kA/cm^2, with a maximum output power and WPE of 9 W and 29.3%, respectively. This is close to the predicted WPE of 28.9%. The WPE is maximized at a current density of ~4 kA/cm^2, which is a little lower than that of the laser from Ref. [10] (4.25 kA/cm^2). This is an indication that the laser core doping is ~6% lower than the reference wafer. Some of this is reflected in the J_{th} value, which is 11.6% lower than the reference. The residual decrease is explained fairly well by the lower waveguide loss and increased confinement factor, which was estimated to drop J_{th} by ~4.9%. The inset of Fig. 4(a) shows the spectrum of a QCL with this design at a current density of 2.5 kA/cm^2.

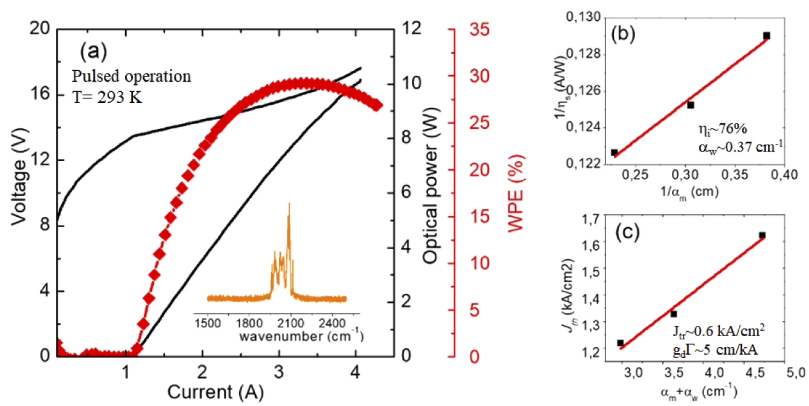

Fig. 4. (a) The LIV curves and extracted WPE for a 5 mm long, 17 µm wide laser. Inset: the spectrum of the laser emission at 2.5 kA/cm^2 (b) The mirror loss dependent slope efficiency and (c) total loss dependent threshold current density. These measurements were conducted in pulsed mode with a pulse width of 500 ns and a duty cycle of 2% at 293 K.

Additional measurement of 3 and 4 mm long, uncoated cavities were used to study the laser characteristics as function of mirror loss. The internal quantum efficiency and waveguide loss of the QCL can be obtained from the cavity length dependent experiment by linear fitting on $1/\eta_s$ as a function of $1/\alpha_m$ in Eq. (4).

$$\frac{1}{\eta_s} = \frac{1}{\eta_i} \cdot \frac{e}{N\hbar\omega} \cdot (1 + \frac{\alpha_w}{\alpha_m}) \tag{4}$$

where e is the charge of electron, N is the numbers of QCL stage, $\hbar\omega$ is the energy of one photon and α_m is the mirror loss. Figure 4(b) shows the reciprocal of η_s as a function of the reciprocal of mirror loss. Fitting by Eq. (4), the internal quantum efficiency and waveguide loss are estimated to be ~76% and ~0.37 cm^{-1}. Compared with the reference ($\alpha_w \approx 0.5$ cm^{-1}), the waveguide loss is reduced by ~26%, which matches quite well with the calculation (>27%) in part 2. A similar analysis can be made by studying the change in J_{th} as a function of mirror loss in Fig. 4(c), which leads to estimates for $g_d\Gamma$ and J_{tr} of 5 cm/kA and 0.6 kA/cm^2, respectively. With this additional data, η_v and η_e for the 5-mm QCL are estimated to be ~88% and ~53%.

Another piece of the new wafer was processed to be a narrow, buried ridge QCL with a ridge width of ~8 μm and a cavity length of 5 mm as shown in Fig. 3(d). The back facet of the device is high-reflection (HR) coated with Y_2O_3/Au/Ti and the front facet is anti-reflection (AR) coated with Y_2O_3 dielectric material with the goal of reproducing the mirror loss of a 5-mm, uncoated cavity. This mirror loss was chosen as it exhibited the highest pulsed WPE of all of the cavity lengths experimentally tested in Fig. 4. To efficiently extract heat from the laser core under CW operation, the QCL was epi-layer down bonded on a patterned diamond heat spreader using indium and then mounted on a water-recycled microchannel cooler.

Figure 5 shows the LIV curve (black, dashed lines) of the QCL under CW operation with a water temperature of ~20 °C. The threshold current density is 1.3 kA/cm^2, with a maximum output power of 5.6 W. In Ref. [10], the CW threshold current density of a similar geometry device is 1.38 kA/cm^2. While the pulsed J_{th} difference was 11.6%, the CW J_{th} difference is only 6%, indicating that the 45-stage device has a slightly higher internal temperature, as predicted above. Nevertheless, thanks to a higher pulsed WPE and a lower operating current density, the new wafer still has excellent efficiency in CW operation. The extracted CW WPE is shown in Fig. 5. The maximum WPE reaches 22% in CW operation at room temperature, exceeding the highest previous demonstration of 21%. This is similar to the predicted value above (21.7%), allowing for small differences in temperature and input power density.

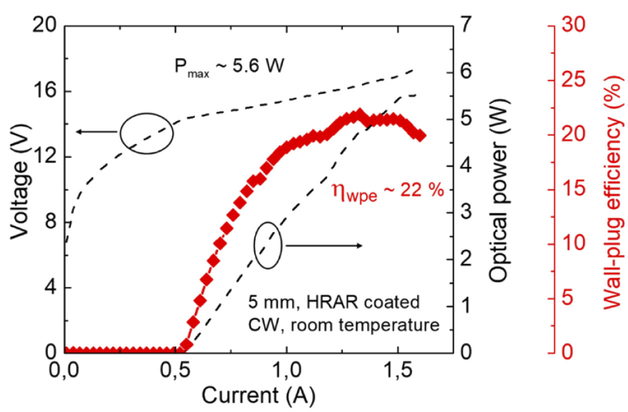

Fig. 5. The LIV curves and extracted WPE of the HRAR coated, buried ridge QCL with 8-μm ridge width and 5-mm cavity length in CW operation at 20 °C.

Further improvements to QCL WPE can be realized by addressing each aspect of laser efficiency. For example, following the same trend, pulsed WPE will definitely be improved by increasing N_s further. However, for better CW WPE, laser geometries with similar core thickness and lower waveguide loss should be investigated. The largest potential impact to WPE will be realized by targeting the laser η_e, which is significantly lower than all other sub-efficiencies. As defined in Ref. [2], this can be achieved by further reducing the laser J_{th} through reduction of J_{tr} and increase of g_d. Just as important is the reduction of parasitic resistance by improving electrical transport efficiency within the QCL active layers.

5. Conclusion

In conclusion, based on a feasibility study using optical and thermal simulations, the WPE of a mid-infrared QCL has been successfully extended to 29.3% at room temperature by increasing the number of emitting stages. With a narrow, buried ridge waveguide and proper packaging, 5.6

Optics EXPRESS

W CW output power was demonstrated for a 5 mm long cavity, corresponding to an extremely high optical density of ~35 MW/cm^2, without damage to the facet. The resulting maximum CW WPE has also been increased to 22%. As the new record of high WPE QCLs, this result extends the efficiency and power capacity of intersubband semiconductor lasers for many important high-power applications at room temperature. In addition, it also demonstrates the technical goal of achieving reproducible material quality for the best QCL wafer design and proves that high efficiency QCLs are a viable technology for manufacturing in future industrial applications.

Funding

Office of Naval Research (N00014-19-C-1049).

Acknowledgments

The authors would like to acknowledge the support and encouragement of following: Dan Green, Kevin Leonard, Myron Pauli, Jason Auxier, Paul Mak, K. K. Law from Navy, and Mark Rosker from DARPA. Any opinions, findings and conclusions or recommendations expressed in this material are those of the author(s) and do not necessarily reflect the views of the Office of Naval Research.

Disclosures

The authors declare no conflicts of interest.

References

1. J. Faist, F. Capasso, D. L. Sivco, C. Sirtori, A. L. Hutchinson, and A. Y. Cho, "Quantum Cascade Laser," Science **264**(5158), 553–556 (1994).
2. M. Razeghi, "High-Performance InP-Based Mid-IR Quantum Cascade Lasers," IEEE J. Sel. Top. Quantum Electron. **15**(3), 941–951 (2009).
3. M. S. Vitiello, G. Scalari, B. Williams, and P. De Natale, "Quantum cascade lasers: 20 years of challenges," Opt. Express **23**(4), 5167 (2015).
4. S. Fathololoumi, E. Dupont, C. W. I. Chan, Z. R. Wasilewski, S. R. Laframboise, D. Ban, A. Matyas, C. Jirauschek, Q. Hu, and H. C. Liu, "Terahertz quantum cascade lasers operating up to ~200 K with optimized oscillator strength and improved injection tunneling," Opt. Express **20**(4), 3866–3876 (2012).
5. M. Razeghi, W. Zhou, S. Slivken, Q. Y. Lu, D. H. Wu, and R. McClintock, "Recent progress of quantum cascade laser research from 3 to 12 µm at the Center for Quantum Devices," Appl. Opt. **56**(31), H30 (2017).
6. Y. Bai, S. Slivken, S. Kuboya, S. R. Darvish, and M. Razeghi, "Quantum cascade lasers that emit more light than heat," Nat. Photonics **4**(2), 99–102 (2010).
7. B. S. Williams, "Terahertz quantum-cascade lasers," Nat. Photonics **1**(9), 517–525 (2007).
8. L. Li, L. Chen, J. Zhu, J. Freeman, P. Dean, A. Valavanis, A. G. Davies, and E. H. Linfield, "Terahertz quantum cascade lasers with > 1 W output powers," Electron. Lett. **50**(4), 309–311 (2014).
9. A. Knigge, G. Erbert, J. Jönsson, W. Pittroff, R. Staske, B. Sumpf, M. Weyers, and G. Tränkle, "Passively cooled 940 nm laser bars with 73% wall-plug efficiency at 70 W and 25°C," Electron. Lett. **41**(5), 250 (2005).
10. Y. Bai, N. Bandyopadhyay, S. Tsao, S. Slivken, and M. Razeghi, "Room temperature quantum cascade lasers with 27% wall plug efficiency," Appl. Phys. Lett. **98**(18), 181102 (2011).
11. Y. Bai, N. Bandyopadhyay, S. Tsao, E. Selcuk, S. Slivken, and M. Razeghi, "Highly temperature insensitive quantum cascade lasers," Appl. Phys. Lett. **97**(25), 251104 (2010).
12. A. Lyakh, M. Suttinger, R. Go, P. Figueiredo, and A. Todi, "5.6 µ m quantum cascade lasers based on a two-material active region composition with a room temperature wall-plug efficiency exceeding 28%," Appl. Phys. Lett. **109**(12), 121109 (2016).
13. Y. Bai, "High wall plug efficiency quantum cascade lasers," PhD dissertation, Northwestern University (2011).
14. J. S. Yu, A. Evans, S. Slivken, S. R. Darvish, and M. Razeghi, "Temperature dependent characteristics of λ~3.8µm room-temperature continuous-wave quantum-cascade lasers," Appl. Phys. Lett. **88**(25), 251118 (2006).
15. D. R. Miftakhutdinov, A. P. Bogatov, and A. E. Drakin, "Catastrophic optical degradation of the output facet of high-power single-transverse-mode diode lasers. 1. Physical model," Quantum Electron. **40**(7), 583–588 (2010).